

SULI RESEARCH PAPER

July 31, 2014

High P_T Jet Analysis Using Monte Carlo Simulation

Kevin Brom
Winona State University
Argonne National Laboratory

Abstract

This paper provides an analysis of high P_T jets for the ATLAS tile calorimeter (TileCal) and liquid argon calorimeter (LArCal). These studies focus on jets with transverse momentum > 650 GeV to better understand how well these calorimeters will perform when the LHC is upgraded for run II experiments at 14 TeV collision energy scheduled for 2015. Using Monte Carlo (MC) simulation, the energy deposition of the calorimeters was investigated for jet P_T up to 3000 GeV. It was found that a higher fraction of the total jet energy is deposited in TileCal as jet P_T is increased whereas energy deposited in LArCal is decreasing slightly. In addition, it was found that energy begins to be deposited deeper into TileCal (BC and D layers) in high P_T jet events. Also, jet energy tends to be deposited more centrally in the barrel region as P_T increases, meaning the extended barrel will see very few, if any, very high P_T jets. This makes the performance of TileCal in the barrel region of paramount importance when studying very high P_T jets in run II.

1 Introduction

ATLAS is one of the major ongoing experiments of the Large Hadron Collider (LHC) in Switzerland. The LHC is currently shut down for upgrades for its run II experiments which will operate at 14 TeV collision energy (run I topped off at 7 TeV) and is scheduled to start back up in 2015. ATLAS has many detectors in it which serve many different purposes. This paper will focus on the calorimeters which measure the energy of particles emitted during collisions. ATLAS has 2 calorimeters which serve different purposes, they are: the Liquid Argon Calorimeter (LArCal) and the Tile Calorimeter (TileCal). Figure 1 shows a cutout of the entire ATLAS detector and the location of the calorimeters. LArCal measures the electromagnetic energy of particles (i.e. electrons, photons) and TileCal measures the hadronic energy (protons, neutrons, mesons). On a very basic level, the LArCal works by an incoming charged particle hitting the liquid argon and ionizing it, then, measuring the resulting signal. TileCal works by converting hadrons into light using a scintillator, then, using a photomultiplier tube, converts the visible light into electrical signals.

Together, the 2 calorimeters can help us study jets. Jets are a phenomena that occur in high energy proton-proton collisions. Protons are made up of quarks (2 up, 1 down) and gluons which bind the quarks (quarks and gluons are known as partons). Each parton has a color associated with it, either red, green, or blue. The color associated with each parton in the proton is unimportant, except that all three colors must be present for it to be stable, or 'color neutral'. When these protons collide though, their partons are released from each other so are no longer color neutral. Colored particles cannot exist by themselves, so partons fragment or 'hadronize' into other particles such as pions or other mesons (quark, anti-quark pairs) until they become color neutral [1]. This hadronization is how jets are formed and can be made of many different particles, which can collectively contain more mass than the original 2 protons. The hadronized particles are what is measured in the calorimeters.

In order to talk more about jets some things must first be understood. First, the coordinate system must be defined. For high energy collisions, a coordinate system consisting of η , ϕ , and P_T is used. η , or pseudorapidity, is defined by:

$$\eta = -\ln\left[\tan\left(\frac{\theta}{2}\right)\right] \quad (1)$$

which is an invariant measurement of the angle relative to the proton beam line ($\eta = 0$ corresponds to an angle perpendicular to the beamline). ϕ is the azimuthal angle; and P_T is defined as:

$$P_T = \sqrt{P_x^2 + P_y^2} \quad (2)$$

which is a measurement of the the transverse jet momentum (momentum perpendicular to the beamline). Knowing these 3 values tells one about jet event kinematics.

A very important aspect in studying high P_T jets is the use of Monte Carlo (MC) simulations. To produce very high P_T jets, very high collision energy is required (higher energies than run I LHC experiments were able to reach). MC simulations are computer algorithms which perform many iterations of random numbers to produce a distribution of numerical values which can then be analyzed. The random numbers are given to quantities which are not well defined, but the behavior of the system can be inferred after many iterations are performed.

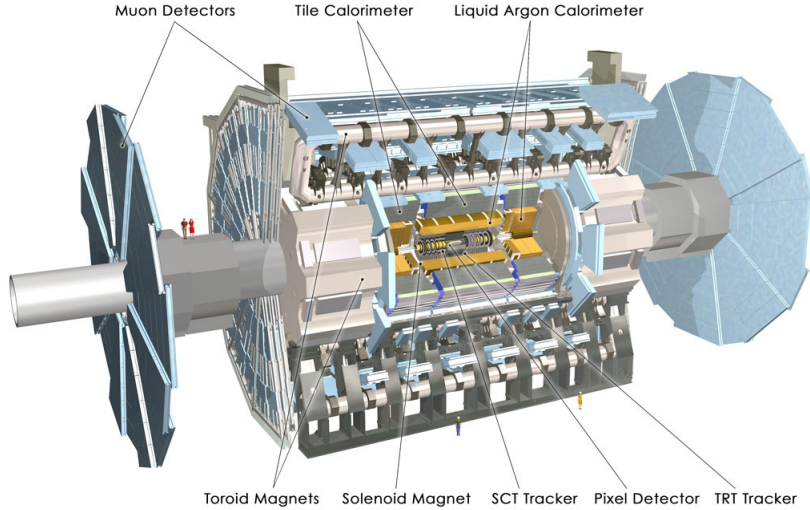


Figure 1: Cutout of the ATLAS detector. LArCal is shown in gold right outside the tracking system, and TileCal is shown in grey right outside LArCal. [2]

2 Energy Deposition in the Calorimeters

It is important to understand how energy is deposited in the ATLAS calorimeters for very high P_T jets because, once the LHC is finished with its run II upgrades, these high energy jets will be heavily studied. In order for them to be studied, it must first be understood how the well detector will handle these events and where potential issues may arise. By using MC simulations we can analyze what one would expect to happen in these high energy collisions. This analysis will help with the calibration of the calorimeters and identify if there is any leakage of energy from the detector that occurs. With the LHC planning to perform at an unprecedented 14 TeV collision energy, this study will help with ensuring that the upgrade performs smoothly.

Using MC simulation, it is possible to see what is expected to happen at these high energy collisions that we otherwise wouldn't be able to see experimentally. The MC simulation used in this study contains physics information to create jet events. The MC simulation used is called PYTHIA8 [3] which simulates LHC proton-proton collisions and contains detector information so it can simulate both what these jet events are expected to produce in reality and how the detector sees the same events. The information about what an event is expected to produce is called truth information, or truth jets; and information about how the detector sees the same event is called reconstructed information, or reconstructed jets. PYTHIA8 was generated to sample different regions of P_T , these are called: PYTHIA8Z4 (Z4), PYTHIA8Z5 (Z5), PYTHIA8Z6 (Z6), and PYTHIA8Z7 (Z7). These simulations can be stitched together to give us information on a wide range of jet collision energies. Specifically, they can provide us with truth and reconstructed information for jets with $650 \leq P_T \leq 3000$ GeV.

The distribution of jet P_T for Z4, Z5, Z6, and Z7 is shown in Figure 2. As can be seen, each simulation has a range of jet P_T 's where most of the jets coincide. When comparing the truth jet and reconstructed jet P_T distribution, Figure 2(a) and 2(b) respectively, it can also be seen that the truth jets have much sharper peaks than the reconstructed jets. This discrepancy can be attributed to the resolution smearing response of the detector. Using Figure 2 as a guide, a range of P_T values can be set to each MC simulation to represent said range. These ranges, using peak to peak values, are: 650-1000 GeV for Z4, 1000-1500 GeV for Z5, 1500-2000 GeV for Z6, and 2000-3500 GeV for Z7. These ranges will be used several

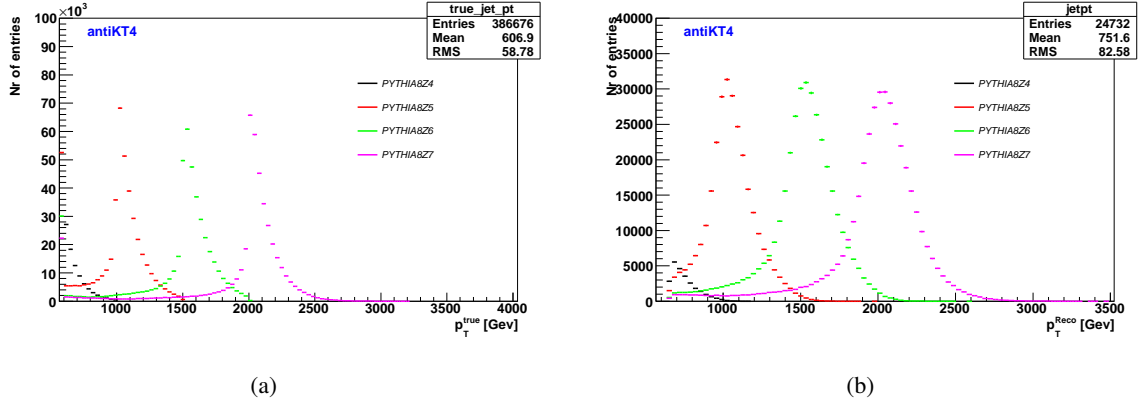


Figure 2: Distribution of jet P_T for truth (a) and reconstructed (b) jets.

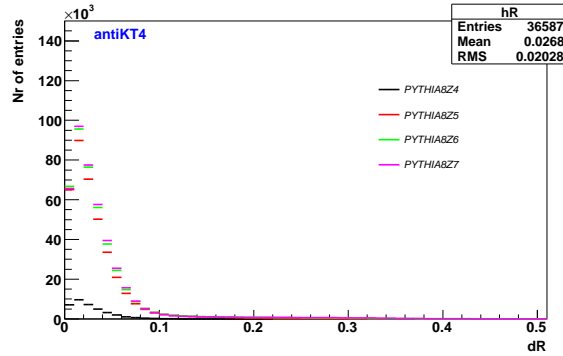


Figure 3: Distribution of dR values for Z4, Z5, Z6, and Z7 simulations. All values are very close to 0 which shows that our algorithm is running with good efficiency. Z4 has much fewer jets here because a P_T cut was made at 650 GeV so many jets are lost as they are not important for this study.

1 times in this research.

2 Next, we matched truth jet information to reconstructed jet information by

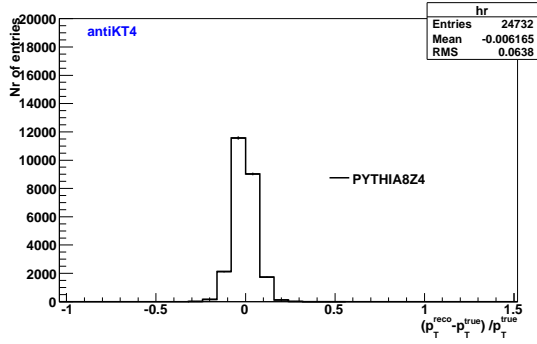
$$dR = \sqrt{(\phi_i^{Reco} - \phi_j^{Truth})^2 + (\eta_i^{Reco} - \eta_j^{Truth})^2} \quad (3)$$

3 and let $dR < .1$. The distribution of dR is shown in Figure 3 which shows most values very close to 0. In
 4 this way, we can ensure that we have close relationship between truth and reconstructed jets. Now that
 5 truth and reconstructed jets are matched to each other, we can check the difference between the 2 jet P_T 's
 6 by the equation:

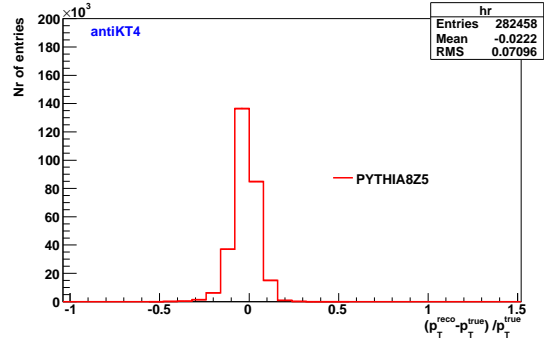
$$r = (P_T^{Reco} - P_T^{True}) / P_T^{True}. \quad (4)$$

7 As can be seen from the distribution of equation 4 in Figure 4, most values have very little difference
 8 between the truth and reconstructed jet P_T values, this is expected because P_T^{Reco} values have already
 9 been calibrated so there should be little to no difference between P_T^{Reco} and P_T^{True} .

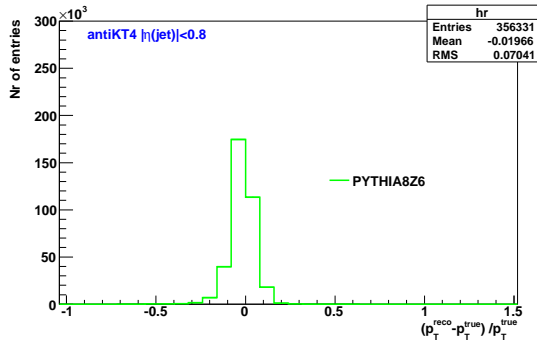
10 Next, we wanted to see how reconstructed information compared to truth information in their ener-
 11 gies. Looking at the reconstructed jet's total energy, electromagnetic energy (as measured in LArCal),
 12 and hadronic energy (as measured by TileCal), it is possible to see the difference of these energies from



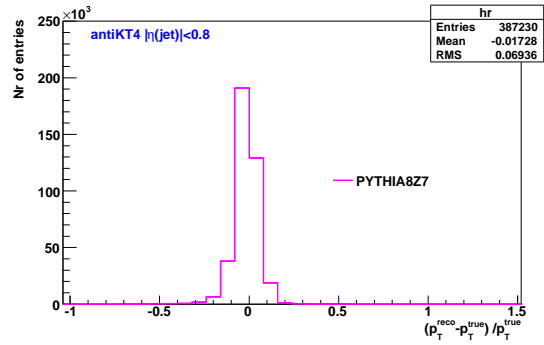
(a)



(b)



(c)



(d)

Figure 4: Distribution of equation 4 values for Z4 (a), Z5 (b), Z6 (c), and Z7 (d). These values are centered around 0 because jet P_T^{Reco} is already calibrated.

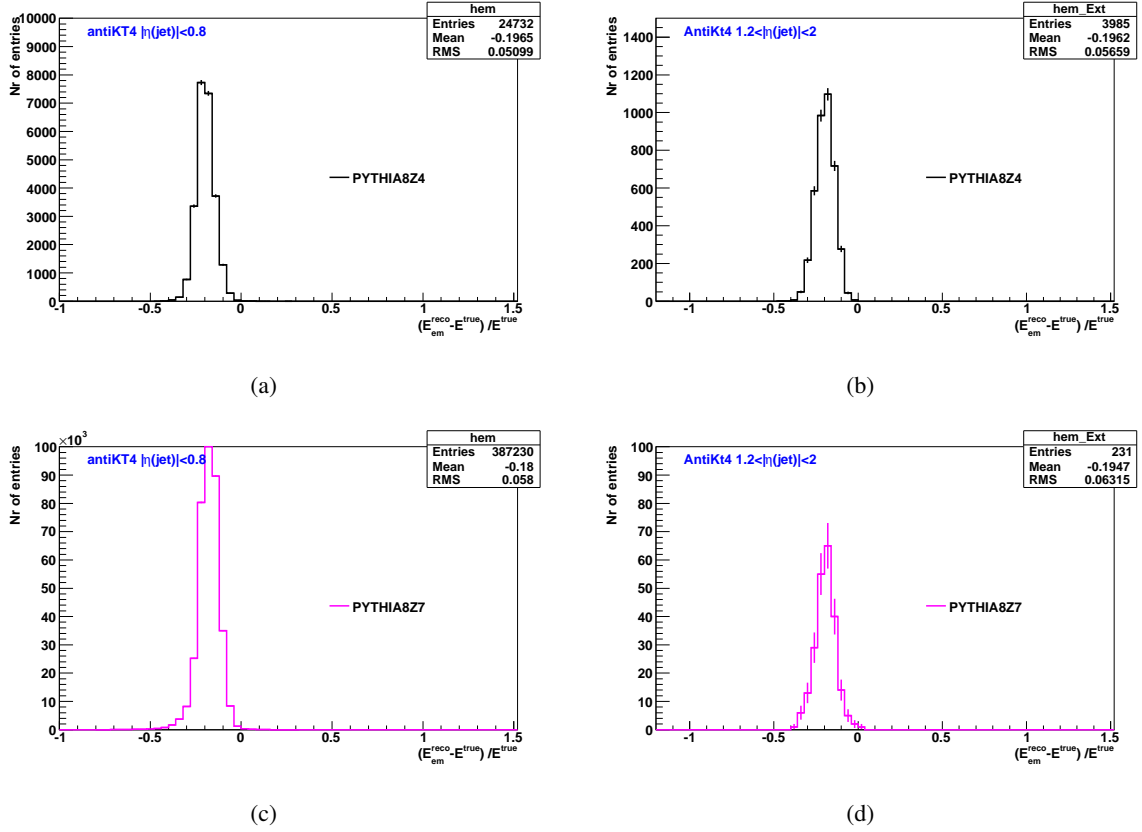


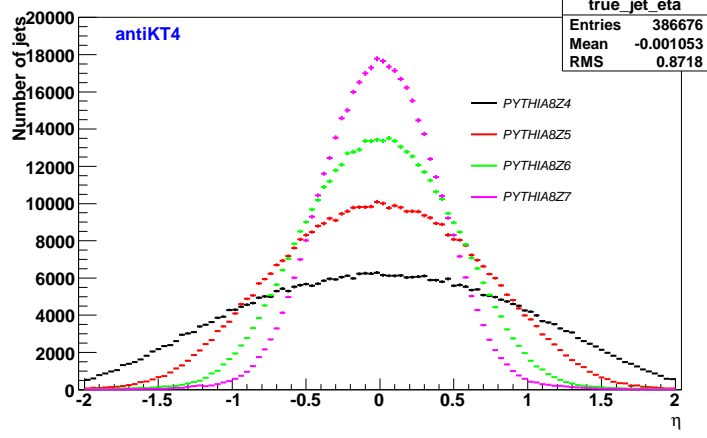
Figure 5: The difference between total truth energy and total reconstructed jet energies at EM-scale for Z4 in the barrel region (a) and extended barrel region (b), and Z7 in the barrel region (c) and extended barrel region (d).

- 1 truth information respectively. The energy detected in these regions is uncalibrated so we say that the
- 2 energy is measured at the electromagnetic scale (EM-scale). Using a similar equation to 4 we can check
- 3 the difference between truth energy and total reconstructed jet energies at EM-scale by:

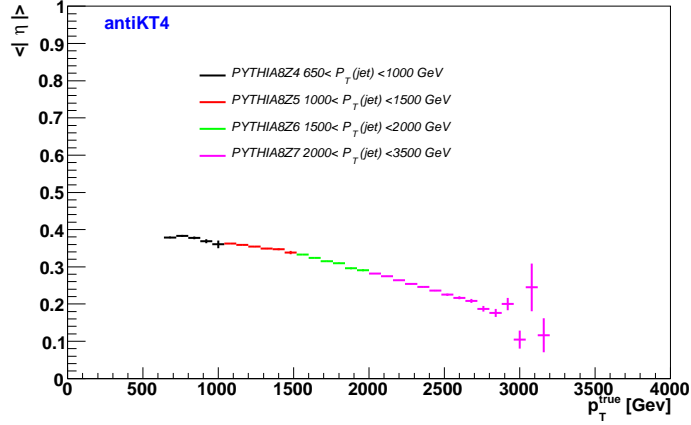
$$r_{em} = (E_{em}^{Reco} - E^{True}) / E^{True} \quad (5)$$

- 4 the distribution of these values can be seen in Figure 5; these figures show lowest P_T and highest P_T
- 5 samples in the barrel and extended barrel regions. Notice that about 20% of the total energy is lost when
- 6 detected, this is due to the fact that the detectors are not perfect and cannot collect all of the energy that
- 7 is actually there.

8 Notice also, in Figure 5 that there are much fewer entries in the extended barrel compared to the
 9 barrel region. This is attributed to the mechanics of dijet events, such that, jets tend to be distributed in
 10 the barrel region ($|\eta| < 1$) of the detector as we move to higher jet P_T . To show that this is a true, Figure
 11 6(a) and Figure 6(b) are included, which shows a distribution of η , and $|\eta|$ respectfully, as a function of
 12 P_T . As can be seen, when we move to higher jet P_T , the jets become more centered around $\eta = 0$. This
 13 means that there are going to be much fewer jets in both the Tile and LAr calorimeters in the extended
 14 barrel region as we get to higher jet P_T . This is an important result because, if high P_T jets are going to
 15 be studied in run II, the barrel calorimeters need to be performing well to capture data from these events.



(a)



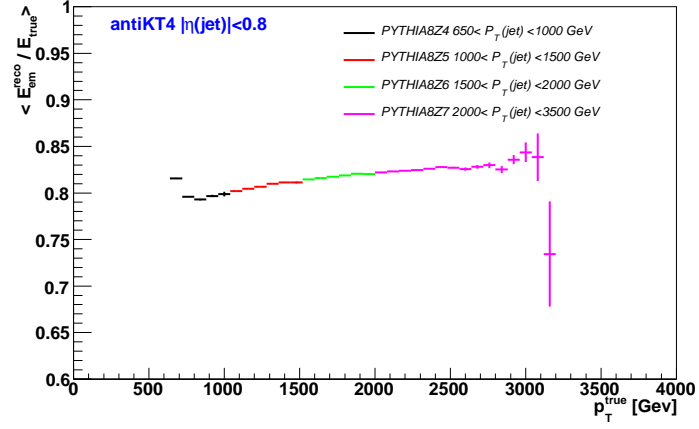
(b)

Figure 6: (a) shows the distribution of jet η values for Z4, Z5, Z6, and Z7 simulations. (b) shows the average value of $|\eta|$ as a function of jet P_T .

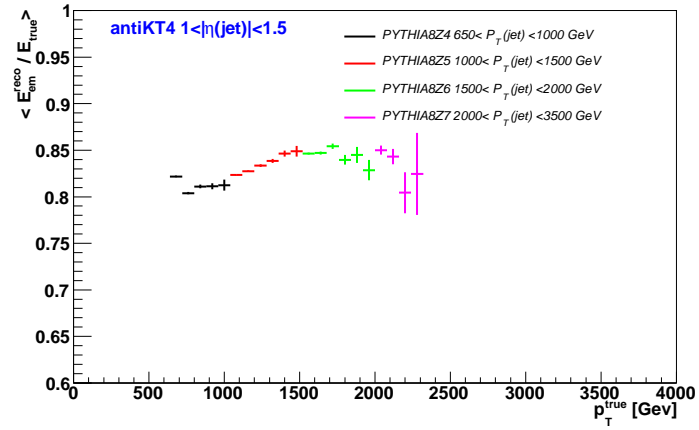
1 Using the ranges specified earlier, we can now look at the ratio:

$$\frac{E_{em}}{E_{True}} \quad (6)$$

2 to see how well the calorimeters perform as we get to higher P_T jets. Average values of equation 6 are
 3 plotted against jet P_T in Figure 7. According to Figure 7, there appears to be no significant leakage in
 4 the barrel region of the calorimeters up to around $P_T = 3000$ GeV. In fact, the calorimeters are seeing an
 5 increase in the amount of total energy they are detecting. Whether this increase in energy is attributed to
 6 electromagnetic or hadronic energy is important to know and will be explored later in this paper. Notice
 7 also, that in the extended barrel there is no information past about 2400 GeV jet P_T . This is a direct
 8 consequence of there being fewer jets in the extended barrel as was discussed earlier.



(a)



(b)

Figure 7: Simulation of average values of equation 6 as a function of P_T^{true} in the barrel (a) and extended barrel (b) regions.

3 Energy Deposition in LArCal

The same analysis that was done for the calorimeters together can also be done on each individually. Looking first at LArCal by the equation

$$r_{LAr} = (E_{em}^{LAr} - E_{True})/E_{True} \quad (7)$$

the distribution of which can be seen in Figure 8, it can be seen that LArCal detects approximately 40-50% of truth level energy. Since the calorimeters detect about 80% of the total energy, this 40-50% detected in LArCal is reasonable since more energy should be captured here than in TileCal because there should be more EM energy than hadronic.

Using the same ranges and a similar method as before we can now look at the ratio:

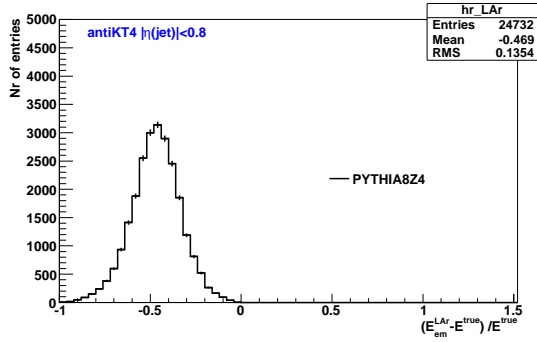
$$\frac{E_{em}^{LAr}}{E_{True}}, \quad (8)$$

to see how well LArCal performs with higher P_T jets. As can be seen in Figure 9, which shows the average value of equation 8 as a function of P_T , the mean energy detected in LArCal at EM-scale is at about 50% lower than the truth energy for all simulations. This energy also seems to be decreasing slightly as we move to higher jet P_T . This could indicate that some energy is being leaked out of LArCal and not being detected. This question will be explored further but one thing is certain at this point: the increase in total energy detected in the calorimeters is not associated with electromagnetic energy measured in LArCal.

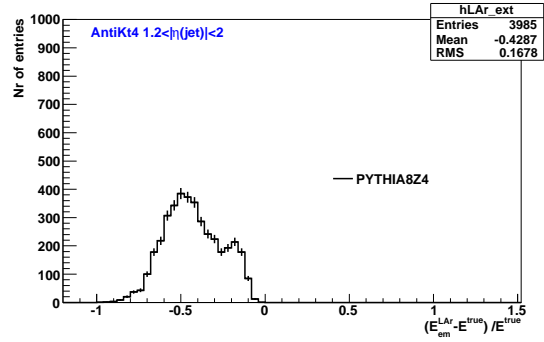
To know where energy is being deposited in LArCal we can separate it into different layers and look at each individually. The layers in LArCal are labeled: 1, 2, and 3 which correspond to the inner-most, middle, and outer-most layers respectfully. LArCal has non-uniform geometry in its 3 layers, Figure 10 shows the material distribution of these layers. Notice layer 3 is the thinnest but gets thicker near the end of the barrel region ($0.4 < |\eta| < 0.8$). So, to determine the energy distribution in LArCal we separate it into 9 different sections: 3 layers in each of the pseudorapidity ranges of ($0 < |\eta| < 0.4$), ($0.4 < |\eta| < 0.6$), and ($0.6 < |\eta| < 0.8$). These 9 sections are compared to the total energy measured in LArCal by the equation

$$f_i = \frac{E_{em}^i}{E_{em}^{LAr}}, \quad (9)$$

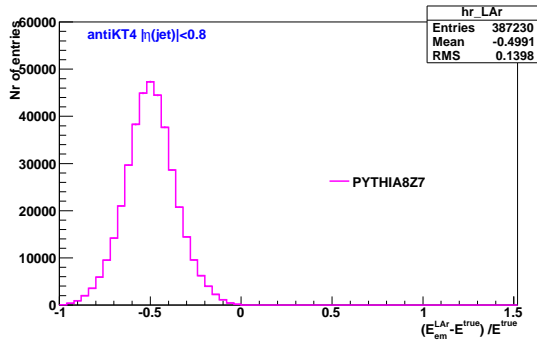
where f_i is the fraction of the total energy in section i , and E_{em}^i is the total energy deposited in section i . These 9 sections are shown in Figures 11, 12, and 13 which correspond to layer 1, 2 and 3 respectfully. As can be seen, as we move to higher P_T , less energy is deposited in layer 1 while more is being deposited in layer 2 for all sections. It's not surprising that layer 2 has the highest energy deposition in LArCal (70-80%) since it is the thickest. Layer 3 is interesting though because of the fact that the thickness is changing the most drastically as we move to the end of the barrel region. Figure 13(a), is the thinnest with 3.3% energy deposition, Figure 13(b) is thicker with 4.5% energy deposition, and Figure 13(c) is the thickest with 7.3% energy deposition. According to these figures it is unclear whether the energy deposition is rising or falling in layer 3 for two reasons: one is that there is not much statistics in this region, and two is that the thinnest section appears to be rising, while the other 2 section of the layer seem to be remaining flat. It is possible for energy to be lost outside of LArCal at very high P_T , or that some hadronic energy is being deposited in this layer but it is not clear exactly what is happenig here. Further research will need to be done to address this question in particular.



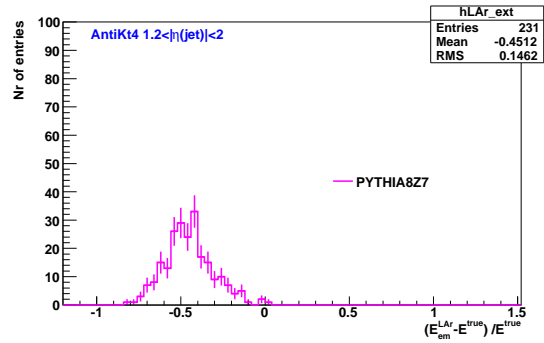
(a)



(b)

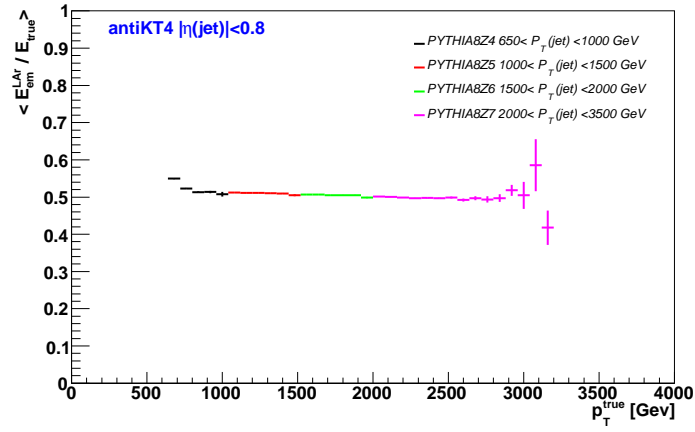


(c)

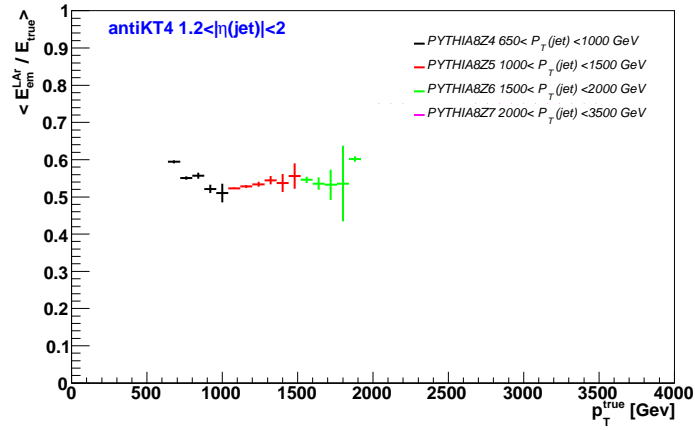


(d)

Figure 8: The difference between total truth jet energy and reconstructed jet energy as seen in LArCal at EM-scale for Z4 in the barrel region (a) and extended barrel region (b) and Z7 in the barrel region (c) and extended barrel region (d).



(a)



(b)

Figure 9: Simulation of average values of equation 8 as a function of p_T^{true} in the barrel (a) and extended barrel (b) regions.

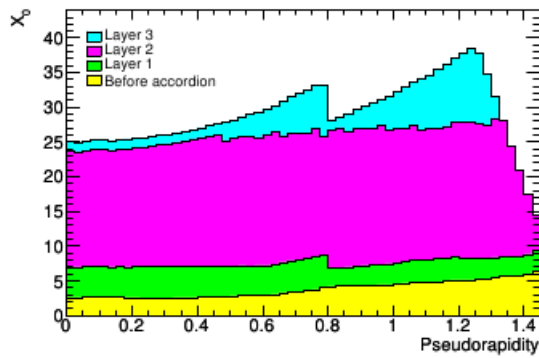
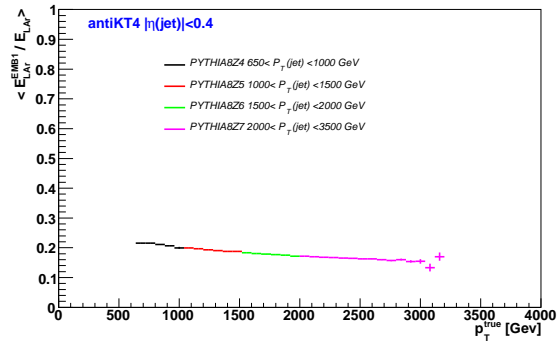
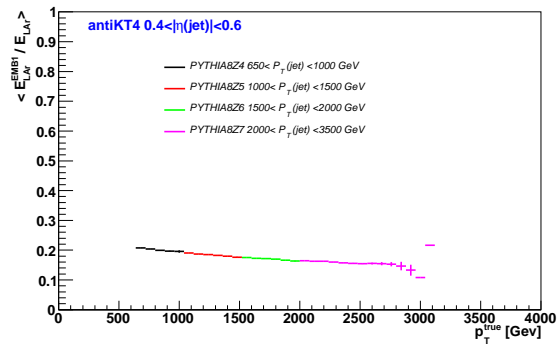


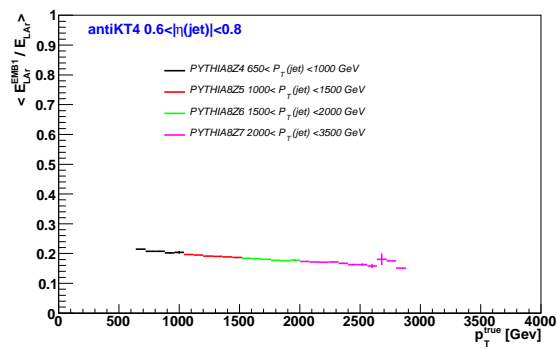
Figure 10: The material deposition in each layer in LArCal as a function of pseudorapidity. [2]



(a)

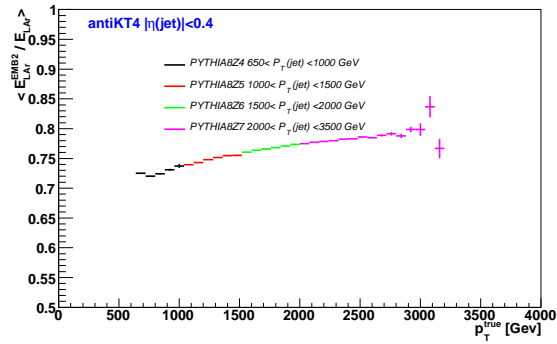


(b)

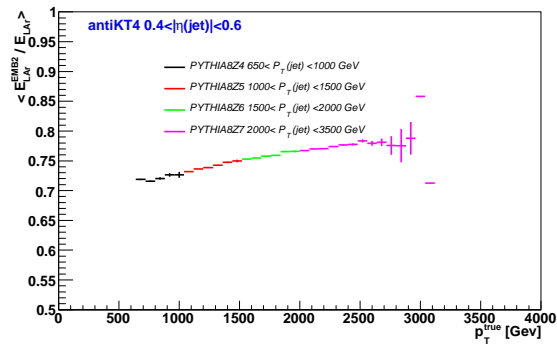


(c)

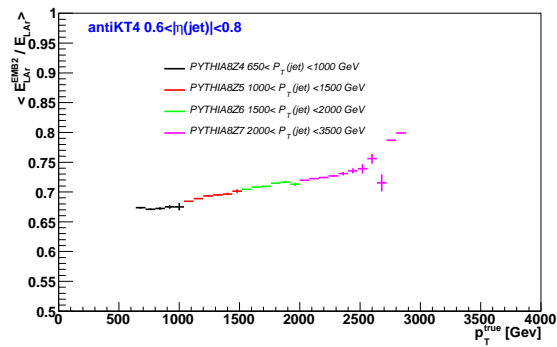
Figure 11: Fraction of energy measured in layer 1 compared to total energy measured in LArCal.



(a)

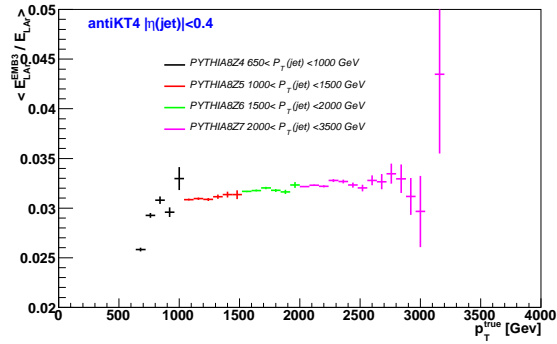


(b)

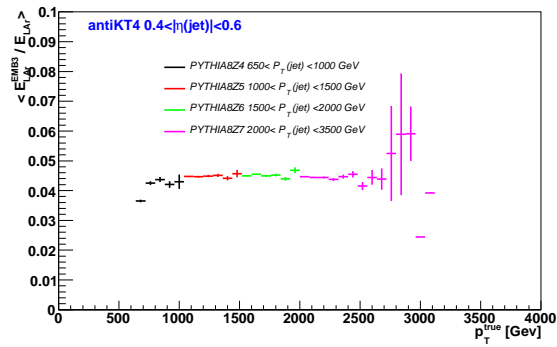


(c)

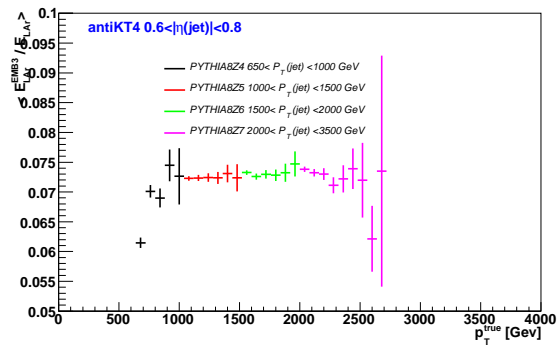
Figure 12: Fraction of energy measured in layer 2 compared to total energy measured in LArCal.



(a)



(b)



(c)

Figure 13: Fraction of energy measured in layer 3 compared to total energy measured in LArCal.

4 Energy Deposition in TileCal

The rest of the jet energy not measured in LArCal should be captured in TileCal. We can do the same analysis done several times before, this time on the TileCal, we have r_{Tile} defined by

$$r_{Tile} = (E_{em}^{Tile} - E_{True})/E_{True}, \quad (10)$$

the distribution of which is plotted in Figure 14. This shows that TileCal loses about 70% of the truth level energy for all simulations. This means that about 30% of the truth level energy is attributed to hadronic energy, as is expected.

Next, we continue using the method used for equations 6 and 8, this time for TileCal by the equation

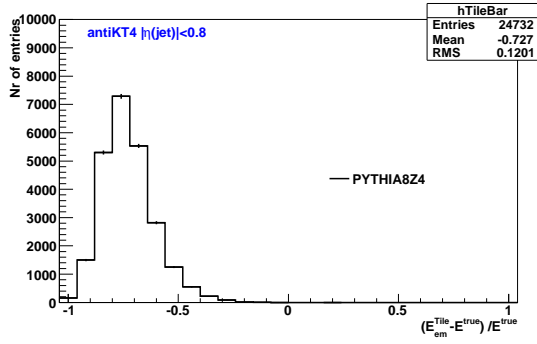
$$\frac{E_{em}^{TileCal}}{E_{True}} \quad (11)$$

we obtain Figure 15. This figure shows that for each simulation, approximately 25% of the jet energy is detected by TileCal and rising to about 35% as we get higher jet P_T . This implies that our overall fractional energy increase is attributed to TileCal measuring hadronic energy. This is an important result because it means that as we get to higher P_T , TileCal's resolution actually increases and we do not see any significant leakage up to 3000 GeV. This also means that TileCal will play an increasingly important role for run II experiments in 2015 with higher collision energies, it could be possible to discover new physics and new high mass particles in these high P_T jets.

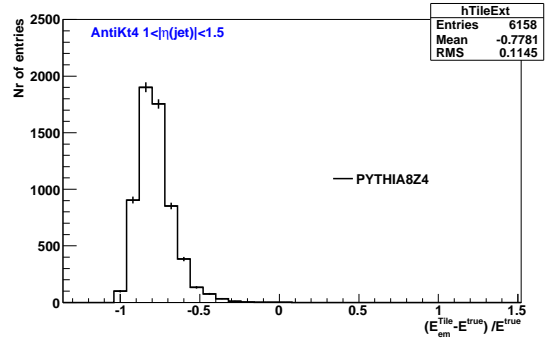
Another important thing to know is how deep jets penetrate into the detector. It is possible to layer the detector into three parts, A, BC, and D. Layer A is the inner most part of TileCal, BC being in the middle, and D the outermost layer. Figure 16 shows the layers of TileCal, since high P_T jets are centered in the barrel region we will only be looking at the barrel layers. Also, since TileCal has a more uniform material distribution than LArCal, sectioning the layers in the detector is not necessary like it was before. To see how much of the energy measured in each layer compares to the total TileCal energy we used a very similar equation to 9. Given this time by

$$f_i = \frac{E_{em}^i}{E_{em}^{Tile}}, \quad (12)$$

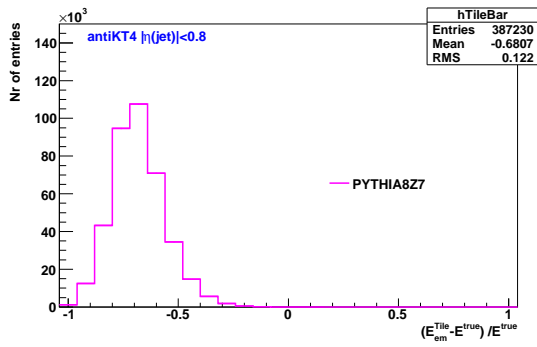
where f_i is the fraction of the total hadronic energy in layer i , and E_{em}^i is the total energy deposited in layer i . Figure 17 plots the average values of equation ?? as a function of jet P_T . Notice, in layer A, how the fraction of energy is decreasing as we get higher jet P_T . This is quite interesting and it is not clear as to the reason behind this fractional energy decrease and should be investigated further. Likewise, the fraction of energy measured in layers BC and D are increasing as P_T increases. From this, we can conclude that jet energy tends to be deposited deeper into TileCal when we have higher P_T jet events.



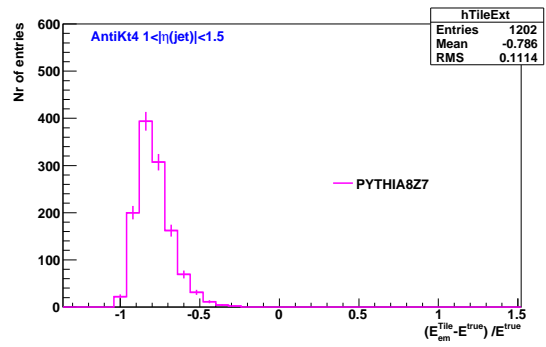
(a)



(b)

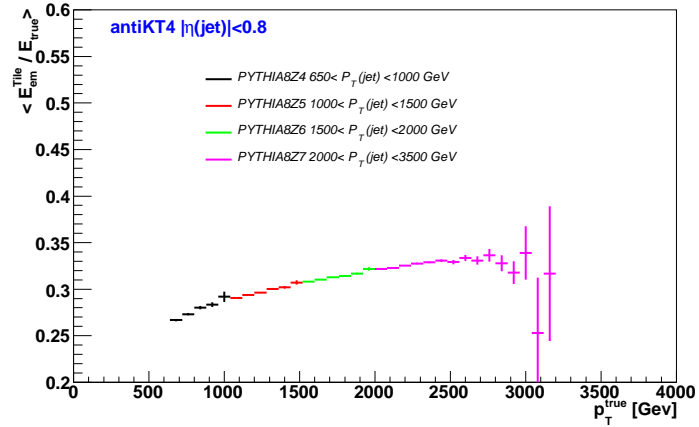


(c)

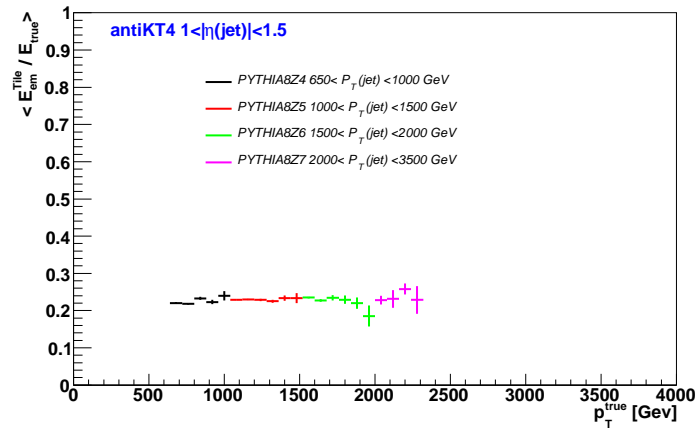


(d)

Figure 14: The difference between total truth jet energy and reconstructed jet energy as seen in TileCal at EM-scale for Z4 in the barrel region (a) and extended barrel region (b), and Z7 in the barrel region (c) and extended barrel region (d).



(a)



(b)

Figure 15: Simulation of the average value of equation 11 as a function of P_T^{True} in the barrel (a) and extended barrel (b) regions.

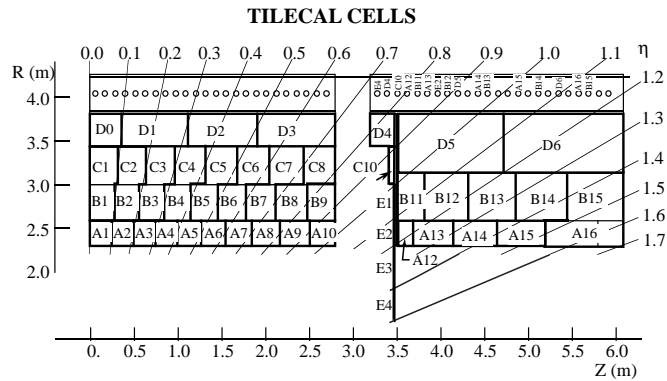
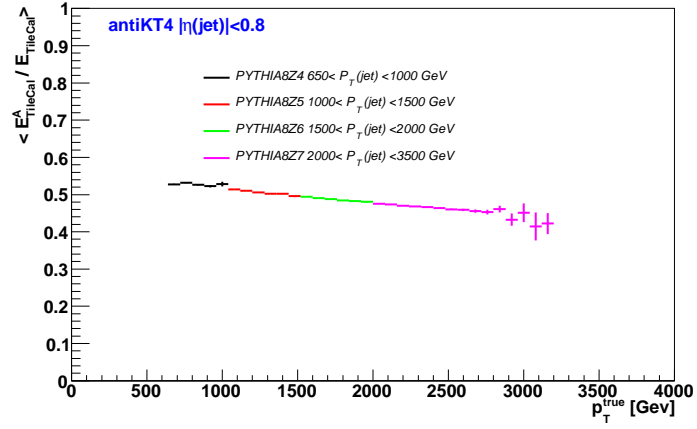
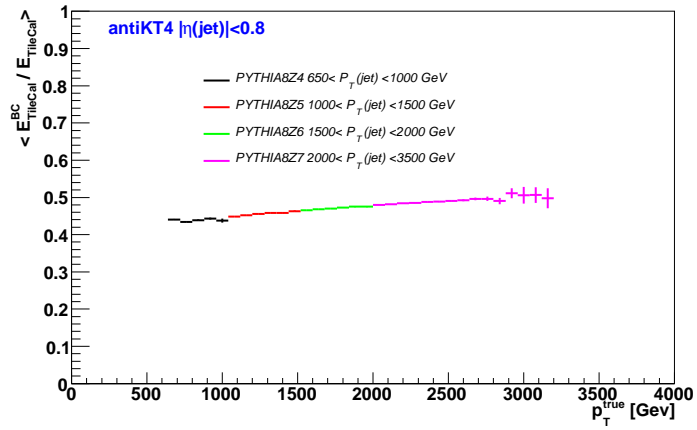


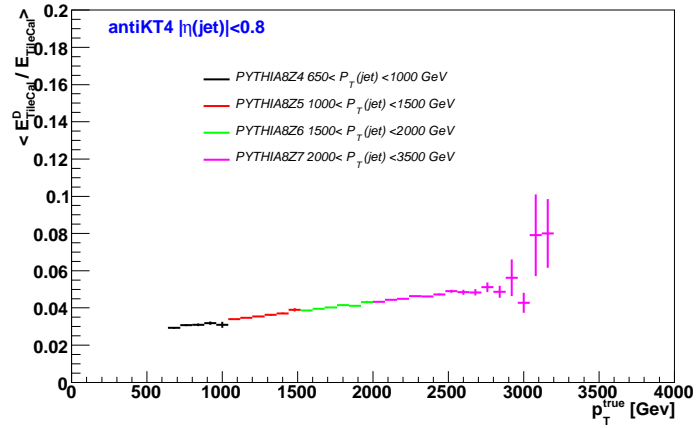
Figure 16: The layers of TileCal in the barrel (left) and extended barrel (right). This analysis focuses on the barrel layers.



(a)



(b)



(c)

Figure 17: Simulation of the average value of equation ?? as a function of P_T^{true} for layers: A (a), BC (b), and D (c)

5 Conclusion

This study reveals some key insight on the performance of the ATLAS calorimeters for run II experiments with high P_T jets. This study was done using the MC simulation PYTHIA8 for jet P_T from 650-3000 GeV.

First, jets tend to be centered in the barrel region as we move to higher P_T leaving very few, if any, in the extended barrel. This indicates that the calorimeters in the barrel region will need to be performing well. Specifically, any dead tiles in TileCal will be detrimental to the analysis of high P_T jets since much of the information from an event would likely be lost.

Second, energy deposition in the calorimeters is shown to be increasing as we move to higher P_T jets. This increase in energy is attributed to hadronic energy as measured by TileCal. Also energy tends to be deposited deeper into TileCal with higher jet P_T . These are important findings because of the possibility of new physics being found using high P_T jets, such as new high-mass particles, dark matter, or dark energy being discovered in these areas and TileCal will play an important role to their discovery.

Third, LArCal seems to be losing a small fraction of energy as we move to higher jet P_T and more investigation will need to be done to understand if there is some leakage out of the outer layer of calorimeter. Energy seems to be deposited deeper into LArCal as we move to higher jet P_T but it is unclear as to how energy is deposited in the outermost layer and more investigation will need to be done to answer this, which in turn, could identify if there is leakage of electromagnetic energy out of this area.

While this research reveals some new things about high P_T jets, it also raises some more questions. First, why does TileCal begin to see an increase in the fraction of energy it detects while layer A is decreasing? Second, why is LArCal seeing a slight decrease in energy deposition as we move to higher P_T ? Also, further research should be done to find out exactly what is happening in layer 3 of LArCal. In addition to these questions, more research should also be done to extend this analysis past 3000 GeV to see if these energy deposition trends continue or change as we get even higher jet P_T .

6 Acknowledgements

I would like to thank Sergei Chekanov, Duong Nguyen, Jermemy Love, and James Proudfoot for helping me grasp some of the complicated concepts of particle physics and answering my constant questions during my 10 weeks at Argonne.

References

- [1] A. Ali and G. Kramer, *Jets and QCD: A Historical Review of the Discovery of the Quark and Gluon Jets and its Impact on QCD*, 2011. Eur. Phys. (2011) 245–326.
- [2] ATLAS Collaboration, G. Aad et al., *The ATLAS Experiment at the CERN Large Hadron Collider*, JINST **3** (2008) S08003.
- [3] T. Sjöstrand, S. Mrenna, and P. Skands, *JHEP05 (2006) 026*, 2008. Comput. Phys. Comm. (2008) 852.